Efficient testing of segmented aspherical mirrors by use of reference plate and computer-generated holograms. I. Theory and system optimization

Feenix Y. Pan and Jim Burge

Telescopes with large aspherical primary mirrors collect more light and are therefore sought after by astronomers. Instead of large mirrors as a single piece, they can be made by use of numerous smaller segments. Because the segments must fit together to create the effect of a single mirror, segmented optics present unique challenges to fabrication and testing that are absent for monolithic optics. We have developed a new method for measuring large quantities of segments accurately, quickly, and economically using an interferometric test plate and computer-generated hologram (CGH). In this test, the aspheric mirror segments are interferometrically measured by use of a test plate with a best-fit spherical surface. The aspherical departure is accommodated with a small CGH that is imaged onto the test plates. The radius of curvature is tightly controlled by maintaining the gap between the test plate and the segment. We present a summary of the test and give the basic design tradeoffs for using a single system to measure all of the segments of a large aspheric mirror. © 2004 Optical Society of America

OCIS codes: 220.4840, 120.3940, 220.0220.

1. Introduction

To collect more light and increase resolution and sensitivity, researchers have expanded tremendous effort in recent years to increase the size of the telescope primary mirrors.[1] Larger primary mirrors give sharper images, since the angular resolution of telescopes is increased. At the limit of diffraction, angular resolution is given by λ/D, where λ is the wavelength of observation and D is the diameter of the primary mirror.

A principle difficulty in the manufacture of a large telescope is the fabrication of the primary mirror. In the case of ground-based telescopes, making monolithic primary mirrors larger than 8 m is unfeasible owing to difficulties of support and transportation. In the case of large-space telescopes when the launch fairings are not large enough, the mirror must be folded during launch. In either case, the primary mirror of a very large telescope must be constructed by smaller segments. Segmenting large primary mirrors into smaller pieces during the mirrors' manufacturing stages allows the construction of an ever-larger telescope. If the segments are manufactured and located perfectly, the optical performance of the mirror is identical to that of a mirror with a continuous surface, except for the light missing from the small gaps between segments.

Segmented mirrors, however, create some unique challenges for fabrication and testing processes. A segmented primary mirror requires that all segments of a primary mirror be correctly phased together to ensure that the mosaic of segments has the same optical shape as an ideal single continuous surface (Fig. 1). Because all segments must perform together to form an optically continuous surface, the tolerance and alignment requirements for each of the segments are much tighter than those for conventional optics. Currently, there is a lack of an established method that can test large quantities of off-axis aspherical mirror segments accurately, quickly, and economically. This paper further develops a new method[2] of testing segmented mirrors that can potentially achieve accuracy and efficiency and be reasonably cost effective.

This paper covers general issues for the test. Section 2 discusses how segmented mirrors tighten the test requirements and summarizes how the system degrades if these requirements are not met. Section 3 describes the new method and shows how it meets

F. Y. Pan co-founded Door-2-Math, P.O. Box 87334, Tucson, Arizona 85754. J. Burge (jburge@optics.arizona.edu) is with the Optical Science Center, University of Arizona, 160 E. University Boulevard, Tucson, Arizona 85721.

Received 17 February 2004; revised manuscript received 5 June 2004; accepted 25 June 2004.

0003-6935/04/285303-10$15.00/0

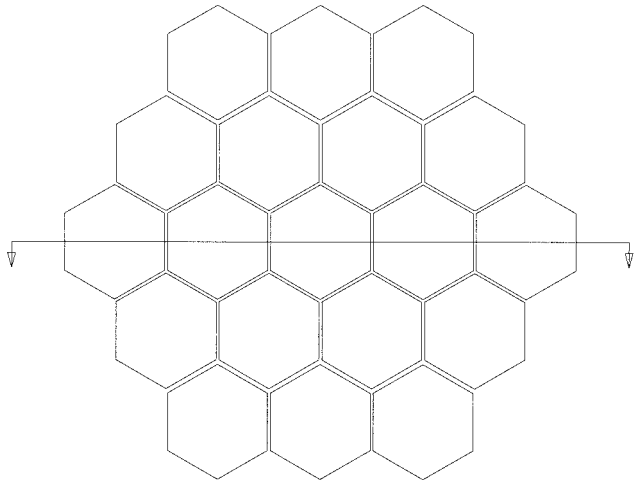

Fig. 1. Mosaic of segments pieced together act as a single continuous mirror, except for the light lost in the gaps.

the necessary requirements for testing segmented primaries. System optimization of the new method is detailed in Section 4.

2. Segmentation Tightens Testing Requirements

The testing of segmented mirrors presents additional challenges that are not present for monolithic optics. Since the segments must fit together, the following parameters must be carefully controlled: piston, tilt, and radius-of-curvature (ROC) matching between segments, translation, and rotation alignment for each segment. In another paper,[3] we carefully examined the effect of these errors on the telescope performance. Here, we only summarize the result in Table 1.

In addition, segmentation requires that each mirror segment be tested quickly. Table 2 shows the upward trend in the number of segments. This means that per-segment measuring time needs to be reduced significantly in order for segmented optics to play a major role in constructing future larger primary mirrors. For example, the proposed California Extreme Large Telescope will have over 1000 pieces compared with 36 pieces for the Keck[4] telescope on Mauna Kea, Hawaii.

3. New Method for Testing Aspherical Segments by Use of a Test Plate and Computer-Generated Holograms

For the reasons listed in the previous section, there is a strong incentive for a new aspherical testing method that can match ROCs to an interferometric accuracy and achieve high accuracy in an efficient manner. Previous research[2] has established the combination of a computer-generated hologram (CGH) with a test plate as a promising technique for measuring large quantities of off-axis aspherical segments. Traditional aspherical CGH tests fail to address the requirements of segmented optics in several ways: 1) a difficulty in establishing relative ROC to an interferometric accuracy, 2) a difficulty in establishing accurate axis location for each segment, and 3) an inefficiency of testing large quantities of segments owing to a lack of built-in alignment accuracy. The new method provides excellent matching of relative ROCs, and is efficient in testing large quantities of off-axis aspherical segments. To summarize, this new method has the following significant advantages:

- High accuracy — achieves $\lambda/100$ rms or better.
- Low cost — requires only one highly accurate spherical reference surface to test all segments.
- Simple to implement — needs minimal vibration/noise suppression owing to its near-common path configuration
- Excellent radius matching — can achieve < 0.010 μm peak-to-valley (PV) power (sag) in surface.
- Accurate axis location — achieves high accuracy in absolute segment placement.

The new test, shown in Fig. 2, measures off-axis aspherical mirror segments using a test plate and CGHs. The test compares a concave mirror segment with a nearly matching convex spherical reference surface of the test plate. CGHs are used to compensate for the aspherical departure of the segment from the spherical reference surface. The test plate reference surface is chosen to be spherical so it can be cost-effectively manufactured and certified to high accuracy. This reference surface is the only high-

Table 1. rms Wave Front as a Function of Alignment/Fabrication Errors[a,b]

Error	Description	Perturbation	Wave-Front Error
Piston	Cophasing of the segments	σ_p, rms piston variation for segment position	$\sigma_{\mathrm{WF}}^2 = 4\sigma_p^2$
Tilt	Copointing of the segments	σ_{tilt}; rms variation for segment tilt	$\sigma_{\mathrm{WF}}^2 = 2\sigma_{tilt}^2$
ROC	Matching the curvature	σ_s, rms sag variation between the segments	$\sigma_{\mathrm{WF}}^2 = \frac{4}{3}\sigma_s^2$
Translation	Segment radial shift	$\sigma_{\Delta b}$, rms variation for segment position	$\sigma_{\mathrm{WF}}^2 = \frac{3}{4}\left[\frac{k^2M^2(M+1)^2}{N}\right]\left(\frac{a}{R}\right)^6\sigma_{\Delta b}^2$
Clocking or rotation	Segment rotation about the local center	$\sigma_{\Delta\theta}$, rms segment rotation (in radians)	$\sigma_{\mathrm{WF}}^2 = \left[9\left(\frac{\sigma_{\Delta\theta}^2}{N}\right)\left(\frac{a}{R}\right)^6(ka)^2\sum_{j=1}^{M}j^5\right]\sigma_{\Delta\theta}^2$

[a] Ref. 3.

[b] σ_{WF}, rms wave-front error; R, primary mirror radius of curvature; a, segment size (half-diameter); k, conic constant; N, total number of segments; M, total number of rings.

Table 2. Large Segmented Telescopes Currently Operational or Planned

Telescope	Primary Diameter (m)[a]	Primary F/#	Number of Segments	Segment Diameter (m) (Across Flat)[b]
Keck[c]	10	1.75	36	1.8
Hobby–Eberly Telescope[d]	10 × 11 hexagon (spherical)	1.308	91	1.0
Gran Telescopio Canarias[e]	10	1.65	36	1.88
California Extremely Large Telescope[f]	30	1.5	1080	1.0
Giant Segmented Mirror Telescope[g]	30	1.0	618	1.335
Euro-50[h]	50	0.85	~618	2.3
OverWhelmingly Large Telescope[i]	100 (spherical)	1.45	~1900	~1.5 to ~1.8
James Webb Space Telescope[j]	6.5	1.25	18	1.3

[a]Aspherical in shape unless otherwise noted.
[b]Equal to the point-to-point dimension of the hexagon.
[c]Ref. 4
[d]Ref. 5
[e]Ref. 6
[f]Ref. 7
[g]Ref. 8
[h]Ref. 9
[i]Ref. 10
[j]Ref. 11

quality surface required for the test, because the test has a near-common path configuration where test and reference beams travel nearly the same optical path. Figure 2 illustrates how this method works:

- The laser beam is first expanded to uniformly illuminate the CGH.
- The CGH is imaged onto the test surface by the projection lens.
- Two CGH diffraction orders, zeroth and first, are selected by placing the object stop at the focal plane of the projection lens.
- The reference beam originates from the zeroth diffraction order of the CGH, reflects off the reference side of the test plate, and then reaches the CCD. The image stop blocks the zeroth diffraction order reflected off the test surface.
- The test beam originates from the first order of the CGH. It has a predistorted wave front that matches the shape of the aspherical mirror segment under test. After reflecting off the test surface, it too reaches the CCD. The image stop blocks the first order of the CGH reflected off the reference side of the test plate.
- The reference and test beams are combined at the reference surface and travel together to the CCD imager. The resulting interference fringes give the shape errors in the mirror segment. The interferogram is imaged onto a CCD array. Adding piezo-

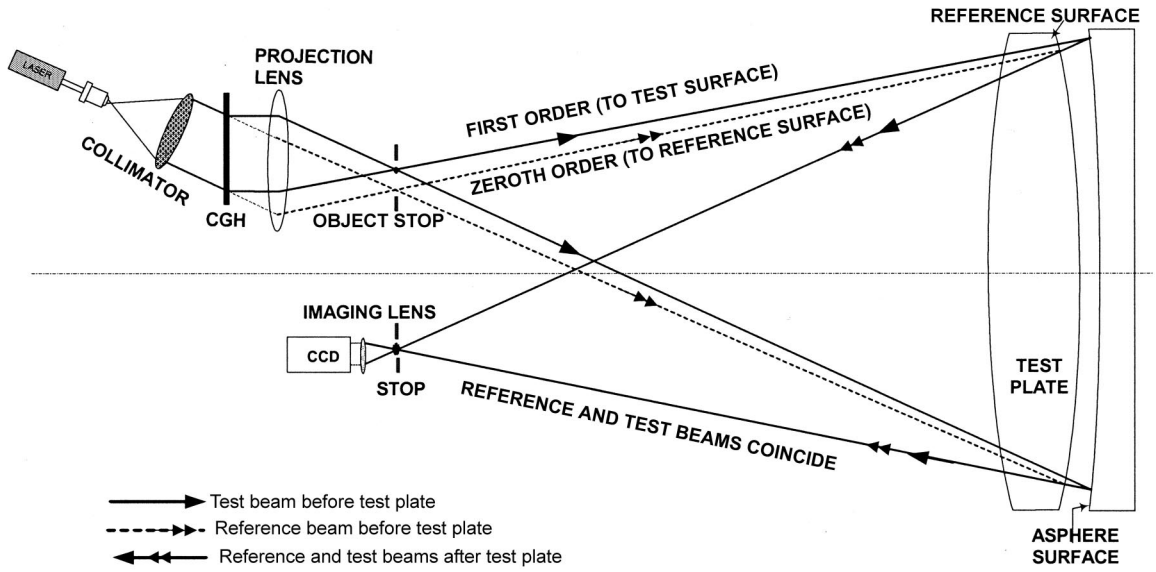

Fig. 2. New test comparing a concave aspherical surface with a convex spherical reference surface of the test plate whose size matches that of the mirror segment. CGH is used to differentiate the aspherical departure of the segment from the spherical reference surface.

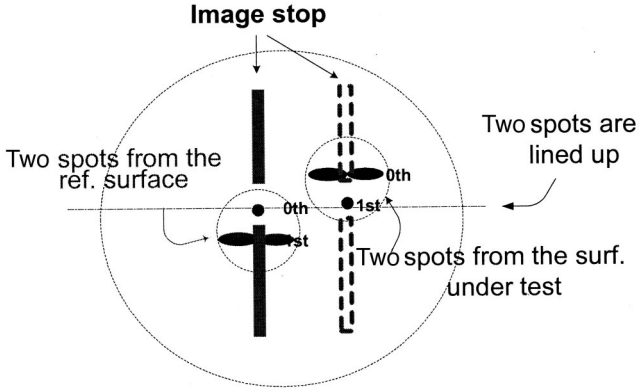

Fig. 3. Orders of diffraction reflected off the two surfaces (aspherical and test plate reference) to give four images. The two orders corresponding to the test and the reference beam are separated by a stop and are coaligned to create interference.

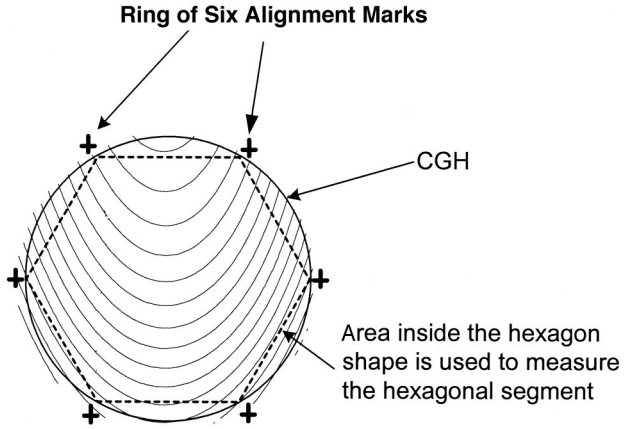

Fig. 4. A ring of six alignment marks etched around the hologram to aid the alignment.

electric transducers to the back of the mirror segment or the test plate allows phase-shifting interferometry.

- The image lens is chosen so that the test surface is imaged onto the CCD.
- An image stop is placed at the front focal plane of the image lens to isolate the appropriate orders (Fig. 3).

This test is ideal for measuring large quantities of off-axis aspherical segments and produces excellent relative ROC matching, since all concave aspheric segments are compared with the same convex spherical reference surface and are maintained by controlling the gap of few millimeters. It is also efficient in that a single test setup can be optimized to accommodate measurement of all segments simply by replacing the CGH. In addition, this method is cost effective; it ensures that both reference and test beams coincide at the CGH, so substrate errors do not affect the test; and it allows the test plate to be made from a nonprecision transmission grade glass, like Zerodur. Finally, by employing phase-shifting interferometry and utilizing its inherent near-common path configuration, this test achieves a high degree of measurement accuracy.

Accurate axis location is achieved by implementing alignment marks on the CGH directly (Fig. 4) and imaged outside side of the segment under test. The position of the projected alignment marks can be measured by use of either a CCD camera or a loupe. The camera or loupe can be aligned with the projected image, and then its position relative to a reference datum on the asphere can be measured.

The holograms are designed with 50% duty cycle, where the opaque lines are half as wide as the spacing. This puts 25% of the incident light into the zeroth order and 10% into the first order of diffraction. The contrast or visibility in the fringe pattern is easily calculated by use of the following:

$$\text{visibility} = \frac{2\sqrt{I_{\text{ref}} I_{\text{test}}}}{I_{\text{ref}} + I_{\text{test}}}, \tag{1}$$

where I_{ref} and I_{test} are the intensities of the reference and test wave fronts.

For measuring bare glass segments, $I_{\text{ref}} = 0.01$ and $I_{\text{test}} = 0.004$, resulting 90% contrast, since

$$I_{\text{ref}} = 4\% \text{ (reflection)} \times 25\% \text{ (zeroth-order diffraction efficiency)} = 0.01, \tag{2}$$

$$I_{\text{test}} = 4\% \text{ (reflection)} \times 10\% \text{ (first; order diffraction efficiency)} = 0.004. \tag{3}$$

The test can also be used to measure aluminized segments. Here $I_{\text{ref}} = 0.01$ and $I_{\text{test}} = 0.095$ (95% reflection and 10% diffraction efficiency), and 58% contrast is achieved. This is still sufficient to allow accurate high-resolution surface measurements.

4. System Design and Optimization

Optimization of the system allows the designer to achieve high testing efficiency while balancing cost and accuracy. When the system is properly optimized, a single test plate with its projection and imaging systems can be aligned once so that all segments can be tested through the insertion of different CGHs. We present a system optimization that allows the test to achieve high measurement accuracy and is cost effective. From the system point of view, there are three independent variables that drive the system design:

- *The reference surface radius of curvature*. This controls the amount of power in the CGH. By optimizing this value, test accuracy and efficiency is achieved. This is discussed fully in Subsection 4.A.
- *The illumination surface radius of curvature*. By carefully choosing this parameter, we can reduce the test length without losing test accuracy. This is dealt in Subsection 4.B.

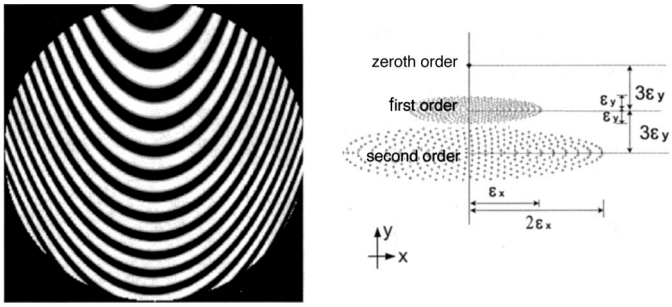

Fig. 5. CGH fringes with a carrier tilt that is three times the maximum wave-front slope of the aberrated wave (left). The first diffraction order is separated in this case (right). Tilt is along the y direction to improve test accuracy.

• *System magnification defined as the ratio of test segment size to the size of the CGH*. Choice of this parameter allows the test to achieve system accuracy and to be cost effective. This is discussed in Subsection 4.C.

A. Optimization of Reference Surface

The test plate is the most critical and the most expensive optical element of this test. One side of the test plate serves as the reference surface, while the other side controls the system illumination. The size of the test plate must match that of the segment under test, making it the largest (therefore most expensive) optical component in the test. Depending on its size, the thickness of the test plate is chosen so that it can be supported to maintain the required figure.

The first parameter that must be chosen for the system design is the ROC of the reference surface. This is selected so that a single test plate can be used for measuring all of the segments and minimizing cost and sensitivity to errors. To understand this selection, we first show how the sensitivity to errors depends on the slope variations compensated by the hologram. Then we show the solution that minimizes these slope variations over the complete set of segments.

The system design must provide a separation between the different orders of diffraction. We use CGH tilt carrier fringes to accomplish this. The minimum amount of carrier tilt required is three times the maximum wave-front slope of the aberrated wave.[12] This condition,[13,14] which must be met whenever a CGH is used, is illustrated in Figs. 5–7. Aberrated wave fronts with large slope variations require carrier tilt fringes that have a higher spatial frequency to separate different diffraction orders.

A limitation in accuracy comes from the hologram fabrication. The magnitude of this effect depends on the spacing. Since tilt carrier fringes dominate the CGH, testing accuracy depends on the carrier frequency. When slope variation of the wave front is asymmetrical, tilt is chosen to be along the direction that has a smaller slope variation. This reduces the sensitivity to errors, since tilt carrier fringes are then not as densely packed. Figure 5 illustrates this point. In this figure, slope variation along the y direction is approximately three times smaller than that along the x direction. CGH tilt carrier fringes are chosen to be along the y direction, so that test sensitivity to CGH fabrication error can be minimized. Figure 6 shows that without any tilt fringes, all diffraction orders, same as those shown in Fig. 5, cannot be separated.

Figure 7 shows that a large amount of tilt must be used to separate orders if they are in the wrong direction. Errors in the diffracted wave front, Δw in unit of waves, due to CGH fabrication errors are given by Eq. (4):

$$\Delta w = \frac{\Delta y}{S_y} m \cong \frac{\Delta y}{\lambda m} \alpha, \qquad \text{since } S_y \cong \lambda \frac{m}{\alpha}, \tag{4}$$

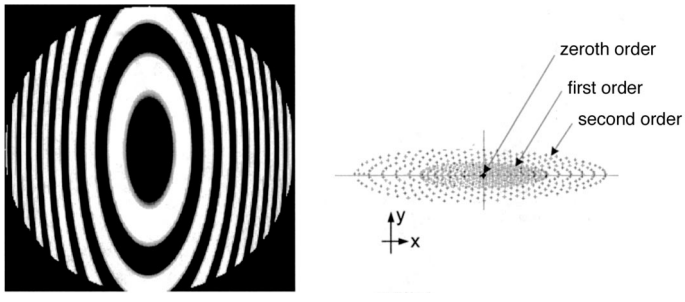

Fig. 6. CGH patterns for the same wave front as Fig. 7 without carrier tilt fringes (left). Diffraction orders are not separated (right).

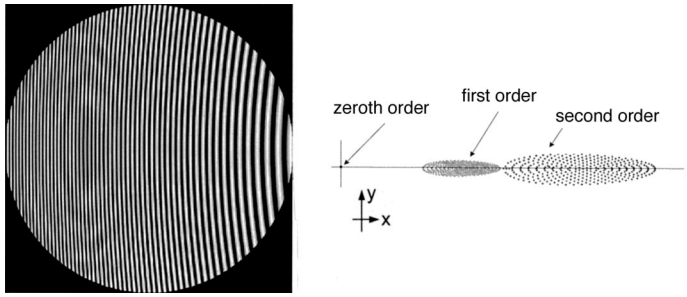

Fig. 7. CGH patterns for the same wave front as Figs. 7 and 8 with carrier tilt fringes in the other direction (left). Diffraction orders are separated in another direction (right). It is apparent that this CGH requires finer spacing and is more sensitive to hologram fabrication errors.

where Δy is the pattern distortion in the direction perpendicular to lines on the hologram, S_y is the center-to-center spacing of CGH lines, α is the diffraction angle, λ is the wavelength of the light used, and m is the diffraction order.

Different reference ROCs correspond to different amounts of power in the hologram. This changes the slope variations of the wave fronts and in turn affects the system sensitivity to CGH errors. The optimal reference surface ROC is selected so that a single test plate can be used for measuring all of the segments and minimizing the system sensitivity to errors. Burge[2] theorized that the optimal reference ROC gives the slope variation of the farthest off-axis segment, matching that of the closest-to-the-center segment.

To locate the optimal ROC value so that a single test plate can be used to test all segments, we developed a computer program that numerically calculates how changes in the reference ROC value affect the slope variations of different segments. Our goal is to choose a single ROC that minimizes slope variation for all of the segments. We choose the specific design for testing segments of an $F/1.0$ 30-m telescope with 618 segments. We denote the innermost segment s1 and the segment farthest from the optical axis s14. The slope variations required for the CGH are plotted, against different ROC values, in the x (radial) and y (tangential) directions in Figs. 8 and 9. Changing the test plate ROC changes the amount of power in the CGH, which in turn changes the slope variation. It is clear from the figures that the minimum slope is found when the ROC that gives the same slope for the innermost and outermost segments is chosen. Also, by comparing Figs. 8 and 9, it is apparent that the slopes are more than twice as small if the optimal is in the tangential direction than if it is in the radial direction. This determines the

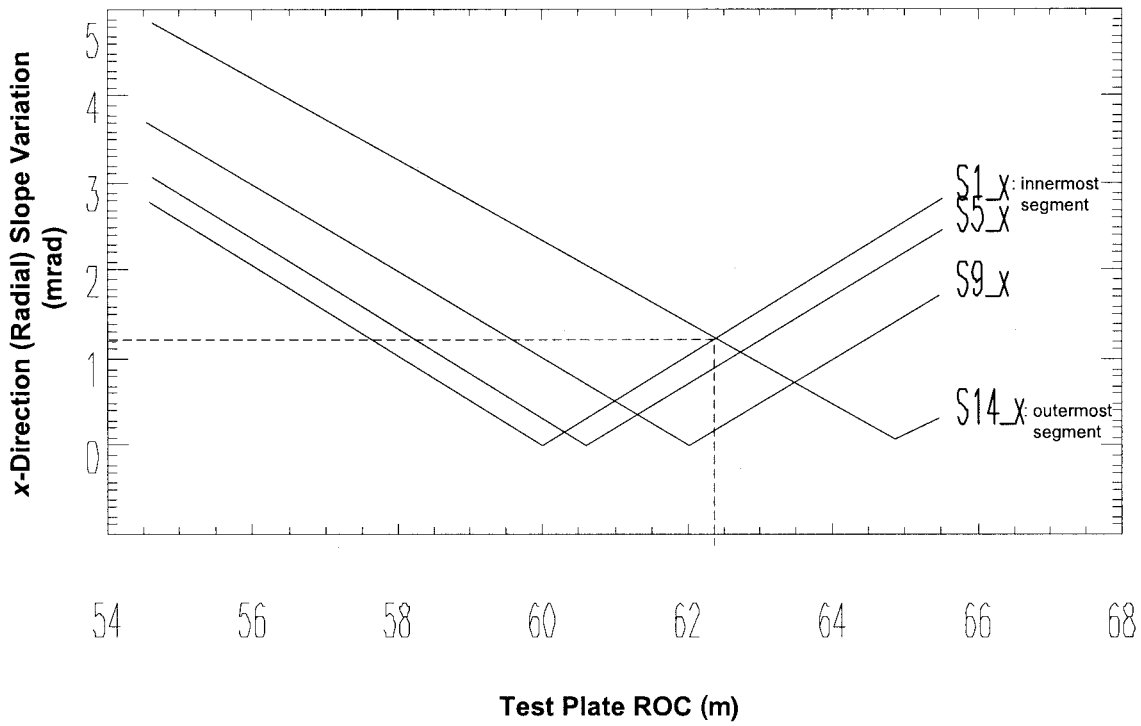

Fig. 8. The x-direction (radial) slope variation of four segments as a function of different reference ROCs in the test plate.

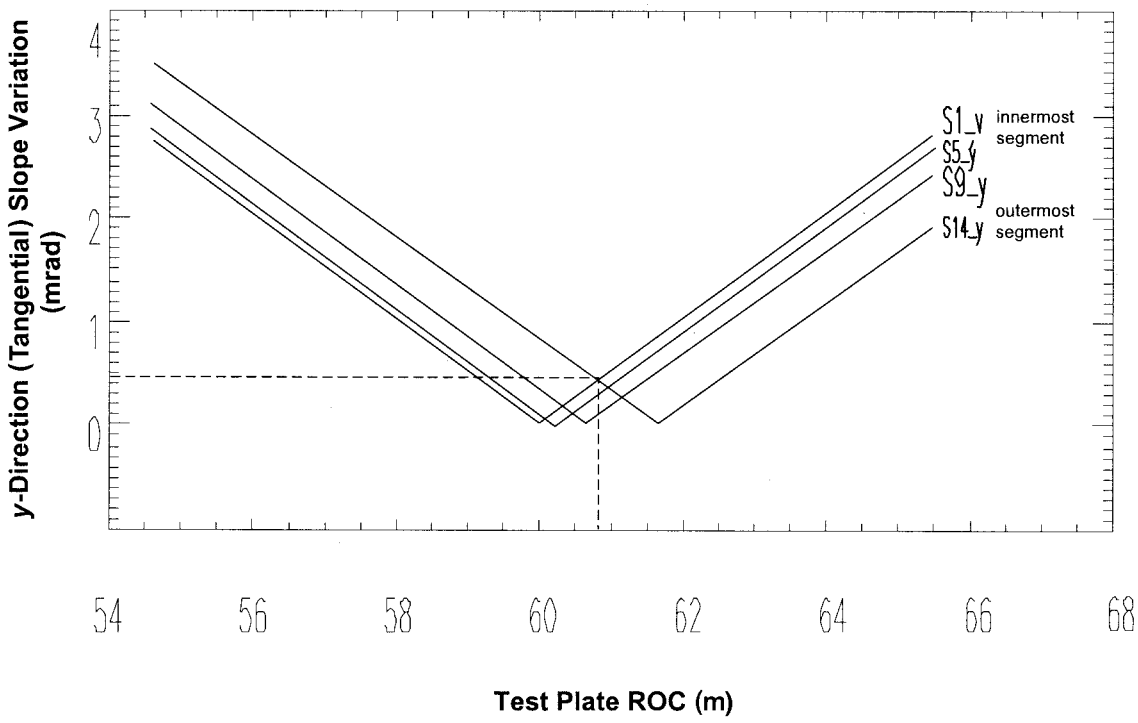

Fig. 9. The y-direction (tangential) slope variation of four segments as a function of different reference ROCs in the test plate.

direction of the tilt fringes on the CGH so that appropriate orders can be separated.

The selection of the optimal reference ROC can be seen in Fig. 10. In this illustration, we plotted slope variations of the same four segments at four different ROC values (lines A, B, C, and D in Figs. 8 and 9). ROC values at lines B and C in Fig. 10 are of interest; on line B, we see that y-slope variations are matched for the nearest segment (S1) and the furthest segment (S14). On line C, we see the same, but now along the x direction. Since test sensitivity to CGH fabrication error is less for smaller slope error, the matched y-direction slope error is used to locate the optimal reference ROC.

B. Optimization of the Illumination System

After optimization of the reference surface ROC, a second component that must be chosen for the system design is the illumination system. The illumination system is designed so that the rays of the reference beam are normally incident to the reference surface. Various detailed designs are well documented elsewhere.[15,16] In designing the illumination system for this test, our main objective is to make the test cost effective, so we designed the entire illumination system using only the test plate's backside, i.e., the nonreference, or the illumination surface.

To be cost effective, the illumination surface is chosen to be spherical. The only design parameter to be chosen is the ROC of the illumination surface. A smaller ROC shortens the viewing distance, measured from the test plate to the object stop, making the test setup shorter. However, a small ROC introduces a higher spherical aberration (SA) into the illumination system. To the first order, SA in the illumination does not affect the test, because it is common in both test and reference beams. However, SA blurs all focused spots at the image stop, and too much SA makes the order separation at the image stop difficult. In addition, the imaging system is easier to design if this aberration is much smaller. Figures 11–13 depict this point. In the absence of SA (Fig. 12), two diffraction orders passed through the object stop (Fig. 11) are easily lined up for interference. When a significant amount of SA is present (Fig. 13), a separation of the orders becomes increasing difficult. From Fig. 13, we conclude that the maximum amount of SA that the system can tolerate is one-third of the separation distance between the zeroth and first orders.

Finally, we note that the illumination surface does not have to be high quality. This is because, aside from a small lateral shear, the test and reference beams nearly coincide on the illumination surface. When both input and output beams co-axial[17] (Figs. 14 and 15), the errors in the illumination-side surface slope can be on the order of $2\lambda/\mathrm{cm}$ (easily achievable), and still yield no more than $0.004\ \lambda$ wave-front error. Note that the layout shown in Fig. 2 uses a lateral shift to separate the return beams. By use of a beam splitter, the test setup can be converted to coaxial.

C. Optimization of System Magnification M

$$M \equiv \frac{\text{segment diameter}}{\text{CGH diameter}}, \tag{5}$$

$$M = \frac{\Lambda}{s} \equiv \frac{\text{fringe spacing at the test surface}}{\text{CGH line spacing}}. \tag{6}$$

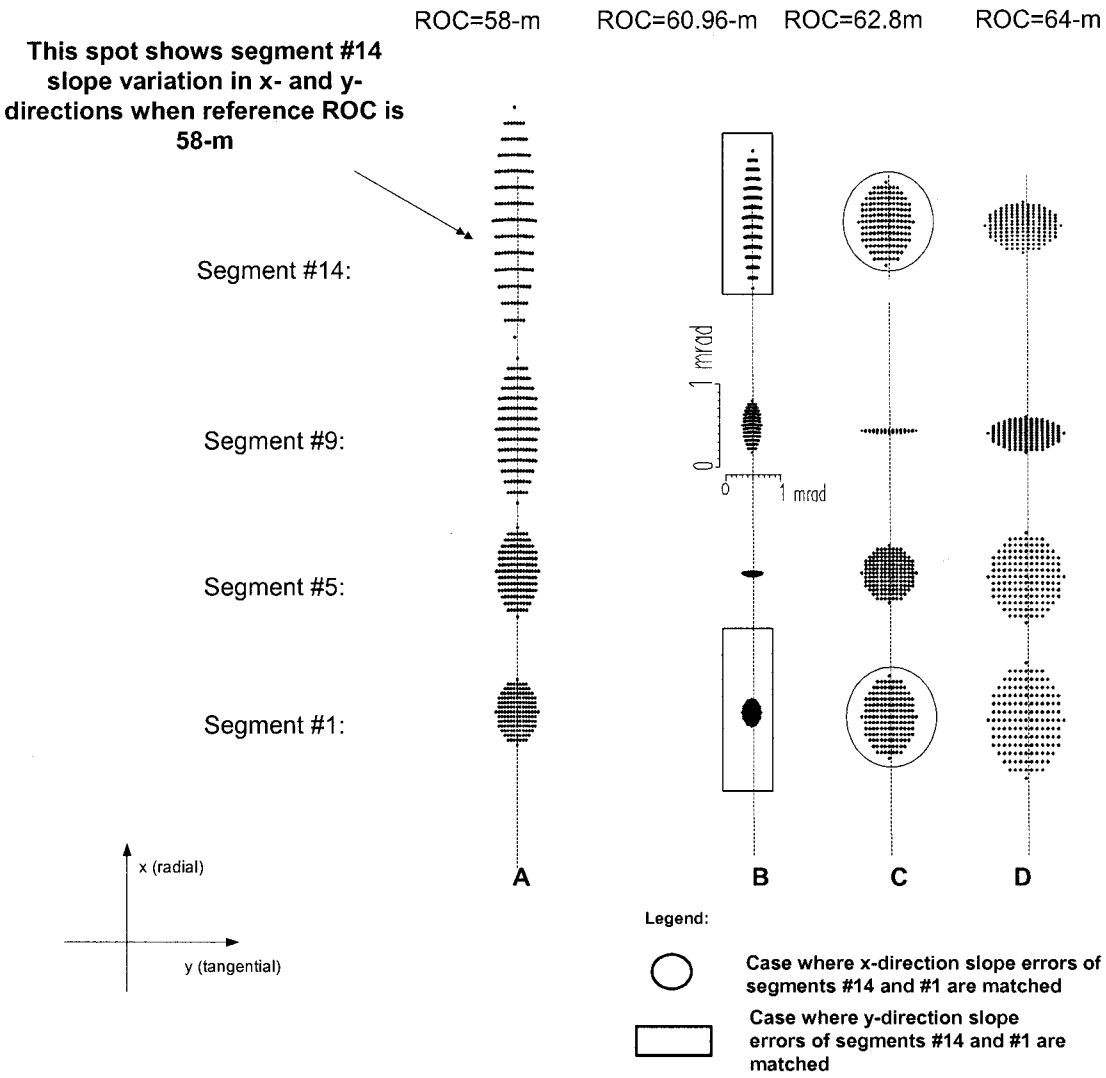

Fig. 10. Spot diagram from the CGH proportional to the slope variation. The optimal system reference ROC is where the slope variation of the farthest off-axis segment (S14) is matched to that of the nearest off-axis segment (S1). Smaller-valued y-directional slope variation is used to locate the optimal ROC, so test sensitivity to CGH fabrication error is reduced. The ROC with the minimum slope variation for the entire set of segments can be seen at ROC = 60.96 m, indicted by line B.

The system magnification M from the hologram to the asphere is the last parameter to be chosen to complete the system design. System magnification M is defined in Eq. (5) as the size ratio of the segment over the CGH. Since the CGH and the mirror segments are conjugate pairs, Eq. (5) is equivalent to Eq. (6), or the fringe spacing at the test surface over the hologram spacing. The fringe spacing at the test surface, measured in λ/mm, is the inverse of the slope difference between the test and reference surfaces, including the carrier tilt. Choice of magnification M changes the CGH pattern spacing, and this affects the test sensitivity to CGH fabrication error. Decreasing M allows for wider CGH line spacing, which improves the test accuracy, but increases the cumulative cost of CGHs because it enlarges the CGH size. The cost for all the CGHs for testing the ensemble of segments can be calculated as a function of the magnification M. The cost of a CGH is peculiar, because it is simply a pattern written on a substrate. The cost of multiple patterns on the same substrate does not increase over the cost of a single CGH. By reducing CGH size, more holograms can be made on the same substrate or at a fixed cost.

However, the smaller CGHs require proportionally smaller periods and are proportionally more sensitive to fabrication errors. The optimal M therefore must balance cost and system accuracy. For example, if we allocate a 2.5-nm surface error for the CGH fabrication error, the minimum pattern spacing should be set to 15 μm [Eq. (7)], assuming laser light with λ of 632 nm is used during the test and CGHs are made with standard accuracy of ± 0.125 μm. We performed a cost-versus-performance study for the cost of the Giant Segmented Mirror Telescope, which requires 103 different CGHs. For this analysis, we assumed that the hologram would be written with ± 0.125-μm ac-

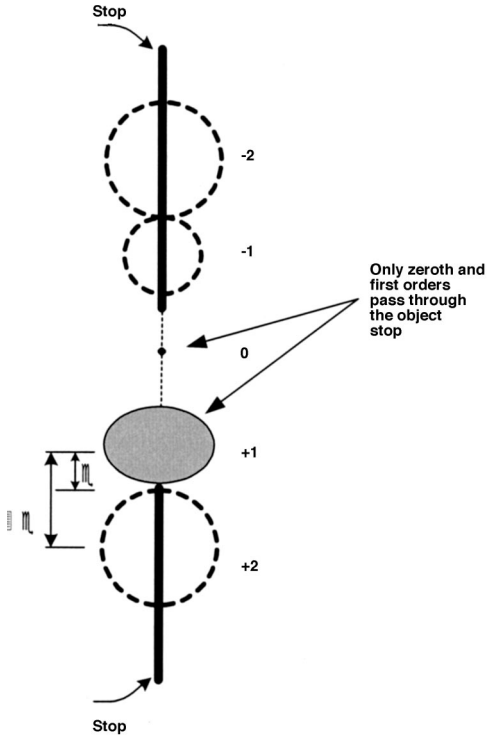

Fig. 11. At the object stop, only zeroth and first orders are passed through.

curacy onto a 15 cm × 15 cm substrate and that the cost per substrate is $10,000.

Figure 16 shows the relationship between CGH fabrication cost and test accuracy.

$$s \geq \frac{0.125\ \mu\text{m}}{2.6\ \text{nm}}\left(\frac{\lambda}{2}\right) \quad \text{or } 15\ \mu\text{m}\,; \tag{7}$$

$$\Lambda = \frac{\lambda}{\sin(\varepsilon_{\text{system}})}\,. \tag{8}$$

To determine the system magnification M using Eq. (6), we first determine the fringe spacing Λ at the test plate. Equation (8) allows us to find Λ using a minimum amount of tilt needed for order separation, $\varepsilon_{\text{system}}$, obtained in subsection 4.A to optimize the

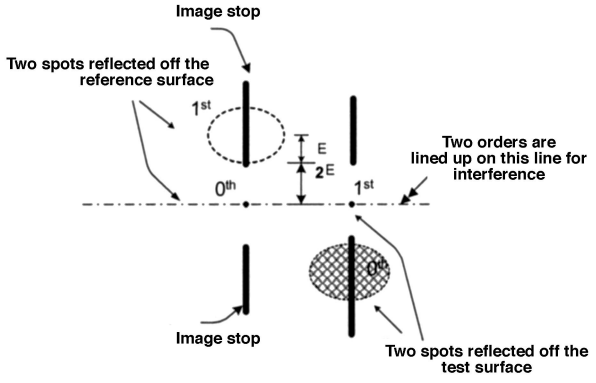

Fig. 12. At the image stop, when SA is absent, appropriate orders are easily lined up for interference.

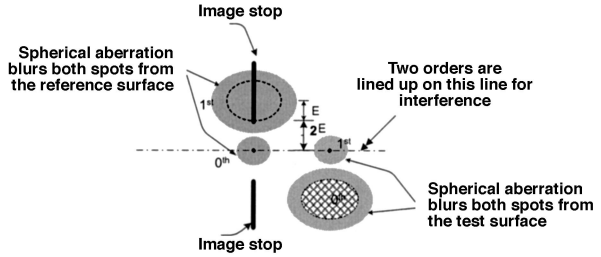

Fig. 13. At the image stop, when SA is significant, appropriate orders that are lined up for interference are blurred. Maximum blur that the system can tolerate is one-third of the order separation distance.

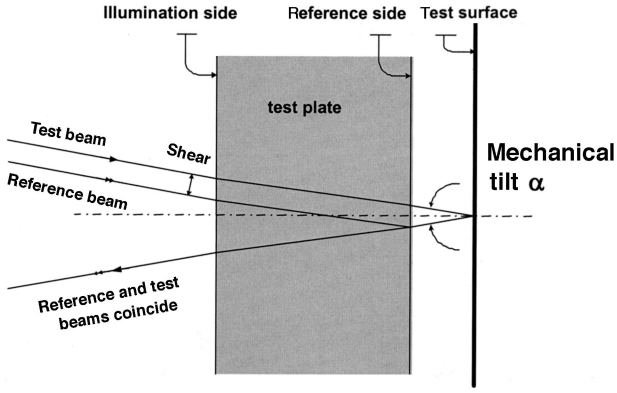

Fig. 14. The input and output beams at the test plate are not coaxial. This causes a shear between the reference and the test beam that tightens the slope requirement of the illumination surface.

reference ROC. From here, with a preallocated error budget for the hologram fabrication error, CGH spacing is found by use of Eq. (7). For instance, for $\varepsilon_{\text{system}}$ of 1.053 mrad and a preallocation of a 2.6-nm rms surface error for a CGH fabrication error, the minimum system magnification is 40× (M = 600.9 μm/15 μm). This requires 33.5-mm CGHs on six 15 cm × 15 cm substrates, which would cost $45,000 for the entire set of 103 holograms.

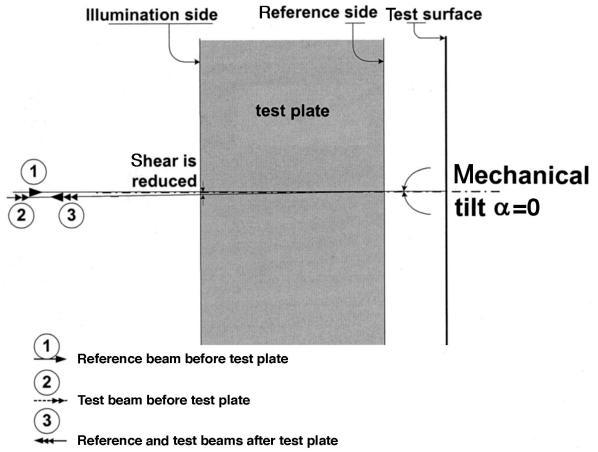

Fig. 15. The input and output beams at the test plate are coaxial. This reduces the slope requirement of the illumination surface.

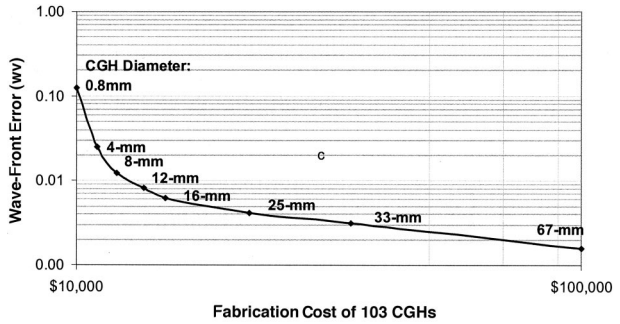

Fig. 16. Trade-off of the cost versus the performance of the holograms required to measure all 614 segments (103 are unique) from a 30-m F/1.0 primary. This assumes that multiple holograms are written onto a standard 15 cm × 15 cm substrate with 0.125-μm accuracy.

5. Conclusion

Combining CGH with a test plate to test large quantities of off-axis aspheres has several advantages, such as low cost, high efficiency, and excellent accuracy. This paper examines the trade-off and the optimization of several important parameters of this method. Validated in the laboratory, this testing method promises an excellent technique for measuring a difficult class of aspheric surfaces.

We thank E. Rudkevich, S. Errico, and D. Anderson for helpful editorial comments and Ms. Gardner for assisting in the preparation of the manuscript. This work is partially funded by the National Aeronautics and Space Administration under contract NGT5-50419, the National Optical Astronomical Observatory under contract C10360A, and the Air Force Office of Scientific Research under contract 49620-02-1-0384.

References

1. J. Nelson, "Design considerations for the California Extremely Large Telescope (CELT)," in *Telescope Structures, Enclosures, Controls, Assembly/Integration/Validation, and Commissioning*, T. A. Sebring and T. Anderson, eds., Proc. SPIE **4004,** 282–289 (2000).
2. J. H. Burge, "Efficient testing of off-axis aspheres with test plates and computer-generated holograms," in *Optical Manufacturing and Testing III*, H. Stahl, ed. Proc. SPIE **3782,** 349–357 (1999).
3. F. Pan, J. Burge, Y. Wang, and Z. Yang, "Fabrication and alignment issues for telescopes using segmented mirrors," Appl. Opt. **43,** 2632–2642 (2004).
4. For more information, see www2.keck.hawaii.edu:3636/gen/info.
5. "Hobby–Eberly Telescope" (University of Texas at Austin, Austin, Tex., 7 January 2004), www.as.utexas.edu/mcdonald/het.
6. "Pagina principal del Proyecto GTC" (Grantecan S. A., La Laguna S/C de Tenerife, Spain, 16 April 2004), http://www.gtc.iac.es.
7. "CELT home page" (California Institute of Technology, Pasadena, Calif., January 2004), http://celt.ucolick.org.
8. "Enabling giant segmented mirror telescope for the astronomical community" (National Optical Astronomy Observatory, Tucson, Ariz., 24 May 2004), www.aura-nio.noao.edu/book/ch4.
9. "Lund Observatory" (Lund Observatory, Lund, Sweden, 9 June 2004), www.astro.lu.se/~torben/euro50.
10. P. Dierickx and R. Gilmozzi, "Progress of the OWL 100-m Telescope Conceptual Design," in *Telescope Structure, Enclosure, Controls, Assembly/Integration/Validation, and Commissioning*, T. A. Sebring and T. Anderson, eds. Proc SPIE **4004,** 405–419, (2000).
11. "James Webb Space Telescope home page" (National Aeronautics and Space Administration, 25 June 2004), http://ngst.gsfc.nasa.gov.
12. J. Pastor, "III. Hologram-interferometry and optical technology," in *New Developments in Interferometry*, H. D. Polster, J. Pastor, R. M. Scott, R. Crane, P. H. Langenbeck, R. Pilston, and G. Steinberg, eds., Appl. Opt. **8,** 525–531 (1969).
13. J. C. Wyant and V. P. Bennett, "Using computer generated holograms to test aspherical wavefronts," Appl. Opt. **11,** 2833–2839 (1972).
14. J. H. Burge, "Applications of computer-generated holograms for interferometric measurement of large aspheric optics" in *Optical Fabrication and Testing*, T. Kasal, ed., Proc. SPIE **2576,** 258–269 (1995).
15. F. Pan, "Measurement of aspherical surfaces using a test plate and computer generated holograms," Ph.D. dissertation (University of Arizona, Tucson, Ariz., 2002).
16. F. Pan and J. Burge, "Efficient measuring of off-axis aspherical segments using a test plate and computer-generated holograms," report submitted to the National Optical Astronomy Observatories (NOAO), July 2002, 950 North Cherry Avenue, Tucson, Ariz. 85721
17. J. W. Goodman, *Introduction to Fourier Optics* (McGraw-Hill, New York, 1968).